A ES
ISSN: 2096-3246
Volume 58, Issue 01, 2026

INVESTIGATION OF CERIUM OXIDE NANOPARTICLES SYNTHESIZED BY CO-PRECIPITATION: A COMPARATIVE STUDY

Pooja Shrivastava[1], Vijay Kumar Baliyan1 and Bhavana Singh[2*]
[1] School of Sciences, Sanjeev Agarwal Global Educational University, Bhopal (M.P.) India, 462026
[2]Department of Applied Physics, Jabalpur Engineering College, Jabalpur (M.P.) India, 482011
poojadeveloped@gmail.com | vkbaliyan2023@gmail.com | *bgodbole@jecjabalpur.ac.in

Cerium oxide nanoparticles were synthesized via a versatile co-precipitation route. The effect of surfactant addition on the structural and optical properties of nanoceria was systematically investigated using X-ray diffraction (XRD), UV–Visible absorption spectroscopy, photoluminescence (PL), scanning electron microscopy (SEM), energy-dispersive X-ray spectroscopy (EDS), and Fourier-transform infrared (FTIR) spectroscopy. XRD analysis confirmed the formation of nanoceria with a cubic fluorite crystal structure, with an average crystallite size of approximately 10 nm. A marginal variation in the optical band gap was observed. FTIR spectra revealed characteristic Ce–O stretching vibrations, confirming the formation of cerium oxide nanoparticles. The PL emission spectra exhibited violet and blue emission bands.
Keywords: Nanoparticles, Cerium Oxide, Co Precipitation, Physical Properties.
Pacs No. 78.55M, 61.05.cp, 78.67bf

1. Introduction

Cerium has atomic number 58 belongs to lanthanide group. It found 0.0046 wt% of earth curst, thus considered to be most abundant [1]. Cerium oxide is electropositive in nature: it has two oxidation states as Ce3+ and Ce4+. Usually Cerium has two types of oxides namely cerium dioxide (CeO2) and dicerium trioxide (Ce2O3). Here cerium dioxide is considered to be more stable. It has wide energy gap approximately 5.5eV [2]. The chemical and physical properties of Ceria nano-crystalline material often contrast from crystalline and amorphous one. CeO2 is thermodynamically stable and having fluorite fd3m structure. This material is transparent in visible region, hence may used for smart windows, electrochemical display, oxygen storage and to filter Ultra violet radiation [3]. Nano-sized CeO2 can have improved dielectric properties, electronic conductivity, lattice relaxation and many more other properties as compared to bulk ceria [4] There are many method for the synthesis of nanoceria like, sonochemical [5], microemulsion synthesis [6], sol-gel process [7], co-precipitation [8] etc. we used simple precipitation method because it is a worthwhile technique which is low cost and efficient way to synthesize materials, particularly oxide materials. This technique permits for the preparation of powders with good flow ability and without the need for additional agglomeration steps with comparative less time. These properties gave utility to this method on industrial level. It also enables growth of controlled particle size and morphology. In present work nanoparticles of CeO2 are synthesized with two different precursor The synthesized particles are analysed using various characterization techniques like XRD, SEM,

ISSN: 2096-3246
Volume 58, Issue 01, 2026

EDS, UV-Visible spectroscopy, FTIR and photoluminescence technique for morphological studies.

2. Experimental Details

The synthesis of CeO2 nanoparticles were carried out with co-precipitation technique. This method's low cost, ease of preparation, and industrial viability has generated a lot of attention. For the synthesis of cerium oxide nanoparticles all chemicals like, cerium (iii) nitrate hexahydrate, hydroxide flakes (naoh), ctab (cetyltrimethyl ammonium bromide), methanol and ethanol are purchased from Taranath chemicals private limited, Warangal, Telangana, India. The double distilled water is used for the preparing suspension and solution.

The first sample is synthesized by taking 0.1 M solution of cerium (III) nitrate hexahydrate (Ce(NO3)3.6H2O) prepared by dissolving 8.7gr, in 0.2L distilled water in one glass jar. Similarly, take 0.2L of distilled water in another glass jar and add 2.4gm of NaOH for preparing 0.3M of NaOH solution. Now drop-wise add solution of NaOH into aqueous solution of cerium (III) nitrate hexa hydrate with constant stirring using magnetic stirrer at room temperature. The pH was maintained at 5 and it takes nearly 150 minute to mix both the solution. Finally, the grey coloured precipitates were obtained in the beaker. Then centrifuge the prepared mixture at 5000 rpm for 30 minute, to get precipitates to settle down at the bottom. After filtering the remaining precipitate were washed multiple times with ethanol and distilled water. Then it was kept as it is till dry then further kept at 150°C for 3hour in a muffle furnace. Finally the dried precipitate was crushed by using motor and pastle.

For preparing second sample, take 250 ml distilled water in a glass beaker, and add 0.1M (10.88gr) of cerium (III) nitrate hexahydrate prepared and 0.05M (4.58gm) of CTAB as surfactant. Similarly, prepare 0.5M solution of NaOH in 250 ml of distilled water and kept in separate beaker. The drop-wise add the solution of NaOH into the mixture of cerium (III) nitrate hexahydrate and CTAB solution with constant stirring by using magnetic stirrer at room temperature. It takes nearly 240 minute to mix both the solution. The pH was checked and found to be 12. Finally pinkish grey coloured precipitates were obtained in the beaker. Then centrifuge the prepared mixture at 1000 rpm for 20 minute, to get precipitates to settle down at the bottom. After filtering the remaining precipitate were washed multiple times with methanol and distilled water. Then it allowed to air dried at room temperature and then further kept at 100°C for 3hour in a muffle furnace. Finally the nanoparticles were obtained by crushing the precipitate by mortar pestle.

3. Result and Discussions

The XRD is a tool for identifying the structural properties of material having nano dimensions. The Bragg's equation is used to show the diffraction from the crystal, given as , this equation allows to find the inter-planner spacing d between the imaginary planes. The so obtained XRD of the prepared samples is shown in fig.1 and fig.2 respectively. The 2 theta vs intensity peaks for sample 1 are located at 2θ = 28.678, 33.23, 47.614, 56.43, 59.16, 69.45 and 76.61 corresponding to (111), (200), (111), (311), (222), (400) and (331) plane. While for sample 2 the diffraction peaks

ISSN: 2096-3246
Volume 58, Issue 01, 2026

located at 2θ =28.610, 33.115, 47.490, 56.37, 59.90, 69.35 and 76.55 corresponding to (111), (200), (111), (311), (222), (400) and (331). The obtained diffraction peaks are well matched with cubic fluorite phase of pure ceria with JCPDS file no. 81-0792 (a=5.4124). Thus, both the samples show the formation of Cerium oxide nanoparticle with cubic fluorite structure with Fm3m space group.

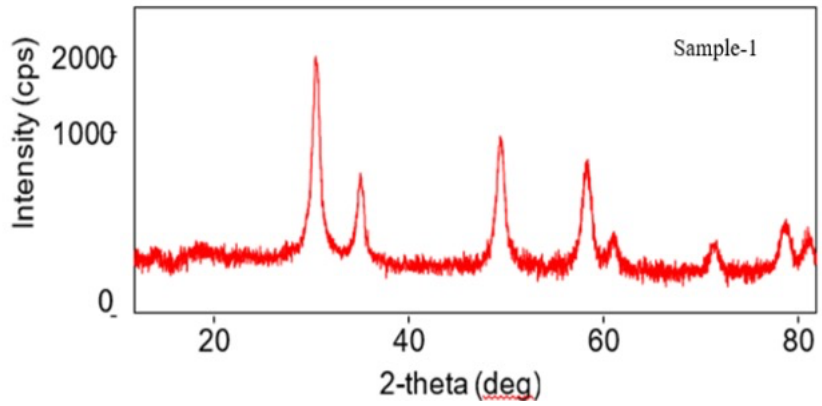

Fig1: X-ray diffraction pattern for sample1

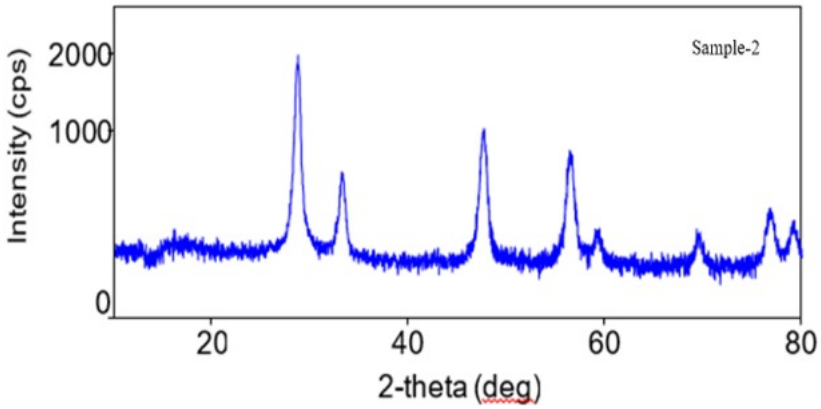

Fig1: X-ray diffraction pattern for sample 2

Debye's Scherrer equation, which reads [9], was applied to determine the crystallite size. In this equation, D stands for mean crystallite size, k for shape factor (0.9), λ for incident X-ray wavelength (1.5418 Å), θ for angle of diffraction, and β for full width at half maximum (FWHM) of the diffraction peak. For the (hkl) plane, the lattice parameter "a" was found using the formula $a=d.(h2+k2+l2)$. The dislocation density δ is [10] described as, , the micro-strain (ε) [11] is defined by formula, , and the unit cell volume (V) is calculated as . The values so obtained are given in table 1.

Sample	Crystallite Size (nm)	Lattice Parameter 'a'	Micro-strain ε	Dislocation Density δ (nm^{-2})	$d_{(hkl)}$ (Å)	Cell volume V	Band gap (eV)	Wavelength λ_{max} (nm)

1	10.147	5.386 Å	0.00834	9.71×10^{-3}	3.116	156.24	4.9	356
2	10.817	5.397 Å	0.00753	8.54×10^{-3}	3.109	157.20	4.7	328

Table 1: crystal structure parameter, band gap and λmax for CeO2 nanoparticle obtained from XRD and Uv-Vis spectroscopy

It has been observed that the crystallite size of sample 2 is slightly higher, where as the dislocation density and micro-strain was found to be reduced as compared to sample 1.The decrease in dislocation density and micro-strain is indicating the decrease in lattice imperfection. It is also observed that strain get reduced due to lattice expansion which is prominent in nanoceria [12].
The absorbance of the material depends on multiple factors like band gap, oxygen deficiency, crystallite size, defects and micro-strain. It also measures the transition of atoms from ground to excited state. We have also carried the Uv-Vis. spectroscopic studies for the absorption range varies from 200 nm to 800 nm by RIGOL 3200 instrument.The fig 3 shows the so obtained absorbance spectra.It shows the abrupt decrease in absorbance up to 248 nm, and then slight increases and reaches the max value to (near ultraviolet region) 352 nm associated with electronic transition. In sample 2 the absorbance decreases minimum around 239 nm, and then slight increases and reaches the max value to (near ultraviolet region) 328 nm. Further increase in wavelength tends to decrease in absorbance of the material.

The measurements of UV-visible absorption spectroscopy could be helpful in elucidating the material's optical band gap energy and electronic structure. Tauc's equation is used to calculate the optical energy band gap [9]: $(\alpha h\upsilon)n=A(h\upsilon-Eg)$, where n is the nature of the optical transition, α is the optical absorption coefficient, h is the Planck constant, ν is the incident photon frequency, A is the transition probability constant, and Eg is the band gap energy. The permissible direct transition is represented by n=2, and the indirect allowed transition is represented by n=1/2. Figure 4 shows, the Tauc plot, by virtue of which the direct energy band-gap was calculated. The direct allowed band gap obtained for sample 1 is 4.9 eV, and for sample 2 it is 4.7 eV [2]. From table 1, it has been observed that the increase in the crystallite size, reduces the absorbance of sample, i.e. the blue shift is observed. This may be due to the fact that smaller particles are responsible for larger surface area, which enhance absorbance. The increment in the band gap energy with decrease in crystallite size is also observed, and this may due to the phenomenon of quantum confinement of ceria. Hence high band gap energy is achieved by sample 1, which has small crystallite size.

ISSN: 2096-3246
Volume 58, Issue 01, 2026

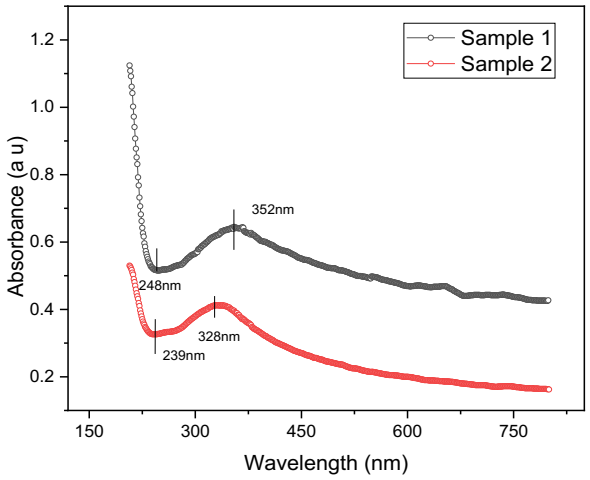

Fig 3: Absorbance Vs Wavelength spectrum for Cerium oxide nanoparticle

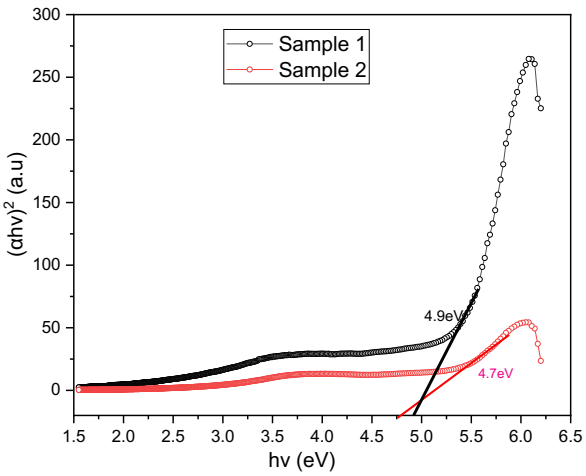

Fig. 4: The plot of $(\alpha hv)^2$ vs hv (eV) for direct transition for sample 1and sample 2

The photoluminescence (PL) spectrum works as an important tool for studying optical and photochemical properties of materials. The optical fluorescence of atoms and molecule in term of intensity versus wavelength is measure by photoluminescence. It is established that, the PL peak intensity is directly related with defect densities, explicitly surface oxygen vacancies present within the materials [13].

A Hitachi 7000 spectrometer was used to record the PL spectra of the CeO2 nanoparticles at an excitation wavelength of roughly 204 nm. Fig 5 and Fig 6 shows, the obtained PL spectra for sample 1 and 2 respectively. For the maximum intense peak obtained in spectra, the direct band gap energy can be calculated by using the relation eV [14].

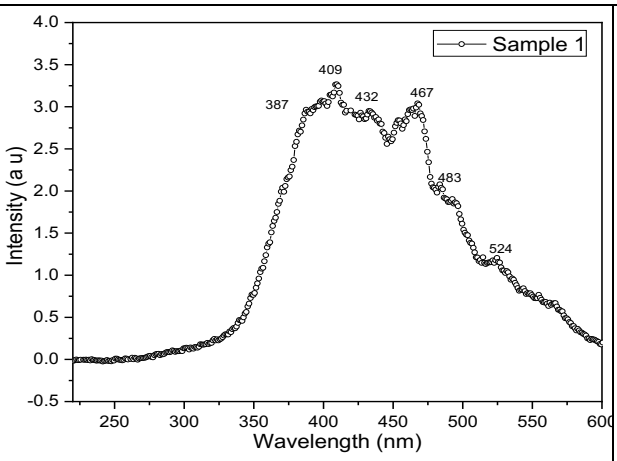

Fig.5:The Photoluminescence spectrum for sample 1.

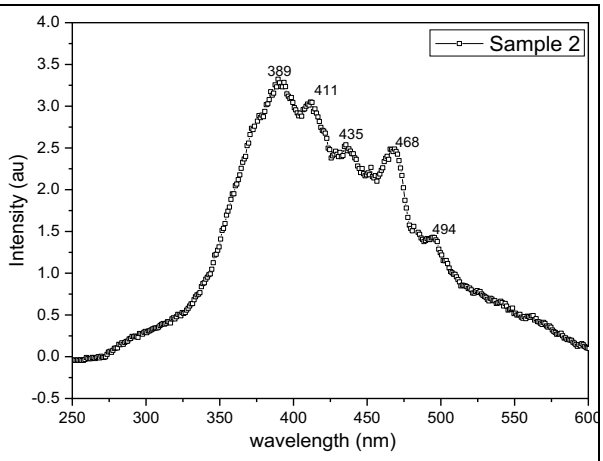

Fig.6:The Photoluminescence spectrum for sample 2.

Sample 1		Sample 2		Emission	Ref.
Wavelength (nm)	Eg (eV)	Wavelength (nm)	Eg (eV)		
387.6	3.199	389.6	3.182	Violet	[15] [16]
409.6	3.027	411.6	3.012		[18]
432.6	2.866	435.6	2.846	Blue	[17]
467.6	2.651	468.6	2.646		
483.6	2.564	494.6	2.507		
524.6	2.363	-		Green	

Table 2: Wavelength with energy band gap (Eg) obtained by PL

Table 2 displays the energy band gap data as well as the peak position obtained in PL spectra. The band-to-band recombination mechanism is responsible for the emission at 387.6 and 389.6 nm [15]. The defect state that is widely distributed between the Ce 4f band and the O 2p band is the source of the violet emission band (409 nm to 411 nm) [16]. The excitonic recombination of CeO2 nanoparticles is responsible for the blue emission bands (432.6, 435.6, 467.6, 468.6, 483.6, and 494.6) [17]. The low density of oxygen vacancies may be the cause of the green emission band (524.6 eV). For the maximum intensity peak, the band gap determined by PL measurement shows the same trend as the UV-Vis measurement result.

The samples are further analyzed using FTIR measurements to identify the type of bond that displays the distinctive vibration bands of both organic and inorganic material, as well as the presence of functional groups. Spectra across the 4000–400 per cm range were recorded. The so obtained absorbance peak found in FTIR spectra are shown in Table 3. The two extra peaks corresponding to 2800-3000 cm-1 are due to presence of CTAB as organic surfactant.

Sr.no	**Sample 1** Wavenumber (cm^{-1})	**Sample 2** Wavenumber (cm^{-1})	**Functional Group/Band Assignment**	**Reference**
1	3431.0	3431.0	O-H bond stretching vibration (absorption of moisture)	[19], [20]
2	-	2926.11	Due to presence of CTAB in sample 2	
3	-	2854.74	Due to presence of CTAB in sample 2	
4	1408.08	1408.08	C-H stretching bond	[19], [21]
5	-	1130.32	C-O bending	[20]
6	1097	1101.39	CO_2assymetric bond	[19]
7	-	1003.02	CO_2assymetric bond	[19]
8	-	895.00	CO_2assymetric bond	[19]
9	-	802.41	CO_2assymetric bond	[19]

10	-	788.91	CO_2assymetric bond	[19]
11	788.91	713.69	CeO_2 bond	[22]
12	-	661.61	Ce-O Stretching	[21]
13	-	634.60	Ce-O Stretching	[21]
14	-	524.66	Ce-O Stretching	[21]
15	-	495.72	Ce-O Stretching	[21]
16	476	468.72	Ce-O Stretching	[21]
17	455	-	Ce-O Stretching	[19], [20]

Table 3: The assignment of absorbance peaks observed in FTIR spectra of samples

The cerium oxide nanoparticles were also analyzed through Scanning Electron Microscope (SEM) and Energy Dispersive Spectroscopy (EDS) measurements. The SEM images (Figs. 7 and 8) of the as-prepared nanoparticles reveal agglomeration of small crystallites, which may be attributed to uncontrolled coagulation during the precipitation process [23]. The micrographs also reveal that the particles are irregularly distributed and exhibit clustered morphology, indicating that the primary nanoparticles underwent aggregation during drying and thermal treatment. The EDS spectra clearly show that the sole elements in the sample are oxygen and cerium. The absence of any additional peaks indicates the high purity and stoichiometry of the synthesized CeO_2 nanoparticles. The weight concentration of Ce and O in sample 1 is 87.38 (error 2.06%) and 12.62 (error 1.44%) respectively, whereas for sample 2 the weight concentration of Ce and O is 82.54 (error 1.71%) and 17.46 (error 1.72%) respectively.

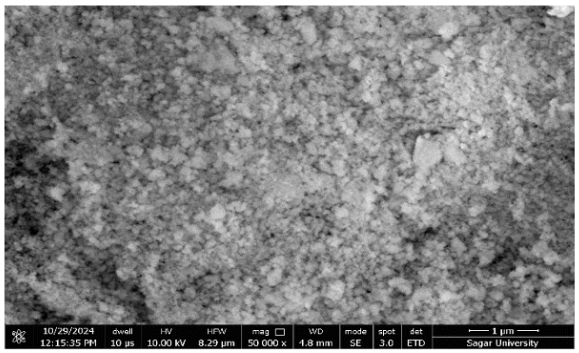

ig. 7: SEM morphology and EDS of nanoceria for sample 1

Fig. 8: SEM morphology and EDS of nanoceria for sample 2

4. Conclusion

Cerium Oxide (CeO_2) nanoparticles were successfully synthesized via a low-cost co-precipitation method with and without the use of CTAB as surfactant. XRD analysis confirmed the formation of highly crystalline CeO_2 with an average particle size of ~10 nm for both samples. The optical band gap energies of 4.9 eV and 4.7 eV indicate only a negligible variation upon surfactant

addition. Photoluminescence studies showed dominant blue emission in both samples. FTIR spectra clearly verified the presence of characteristic O–Ce–O vibrations, confirming the formation of phase-pure CeO_2. The EDS analysis shows impurity-free composition in both cases. The results indicate that the co-precipitation method is suitable for producing stable CeO_2 nanoparticles. A systematic analysis of their structural and optical properties further confirmed that surfactant addition does not significantly alter the fundamental characteristics of the synthesized nanoparticles.

References

1. TizianoMontini, Michele Melchionna, Matteo Monai, and Paolo Fornasiero. Chemical Reviews, 116,10(2016),https://doi.org/10.1021/acs.chemrev.5b00603.
2. Guofeng Wang, Qiuyingmu, Ting Chen and Yude Wang. Journal of Alloys and Compounds, 493 202-207(2010), https://doi.org/10.1016/j.jallcom.2009.12.053.
3. P. N. kalu ,D. U. Onah , P. E. Agbo , C. Augustine , R. A. Chikwenze , F. N. C. Anyaegbunam and C. O. Dike. Journal of ovonic research, 14 293-305(2008),.
4. Adnan Younis, Dewei Chu and Sean Li. Cerium Oxide Nanostructures and their Applications. Functionalised Nanomaterials, (2016), http://dx.doi.org/10.5772/65937.
5. Yu, J. C., Zhang, L. and Lin, J. Journal of Colloid and Interface Science, 260 240-243(2003). https://doi.org/10.1016/S0021-9797(02)00168-6.
6. Muhammad Waqas Iqbal , Yue Yu and David S.A. Simakov. Catalysis Today, 407, 230-243(2023), https://doi.org/10.1016/j.cattod.2021.11.029.
7. AyadShalaga Fudala , Waffa Mahdi Salih and FatinFadhel Alkazaz. Materials Today Proceddings, 49 , 2786-2792(2022), https://doi.org/10.1016/j.matpr.2021.09.452.
8. Paochi Chen., Materials Sciences and Applications, 13, no.4,213-231, (2022). DOI: 10.4236/msa.2022.134012
9. Sara Samiee, Elaheh K. and Goharshadi, Materials Research Bulletin,47 1089-1095 (2012), https://doi.org/10.1016/j.materresbull.2011.12.058.
10. InduVashistha and Sunil Rohilla. IOP Conf. Series: Materials Science and Engineering, 872, 012170(2020). DOI: 10.1088/1757-899X/872/1/012170.
11. Bhavana Singh, S. B. Shrivastava and V. Ganesan. International Journal of Nanoscience, 16, 1650024(2017), https://doi.org/10.1142/S0219581X16500241.
12. Manju Kurian and Christy Kunjachan, Int Nano Lett., 4 ,73–80(2014),https://link.springer.com/article/10.1007/s40089-014-0122-7.
13. Md.A. Subhan, Tanzirahmed, M.R. Awal and B Moonkim. SpectrochimicaActa Part A: Molecular AndBiomolecular Spectroscopy, 135 ,466– 471(2015),
14. Zamiri R, Ahangar H A, Kaushal A, Zakaria A, Zamiri G and Tobaldi D, PLoS ONE, 10 (4) 0122989 (2015), https://doi.org/10.1371/journal.pone.0122989.
15. Zhen Wang, Qi Wang, Yuchao Liao, Genli Shen, Xuzhang Gong, NingHan, Haidi Liu and Yunfa Chen., ChemPhyChem, 12 ,2763-2770(2011), https://doi.org/10.1021/cm991089e.

16. A.H. Morshed, M.E. Moussa, S .M. Bedair, R. Leonard, SX Liu and N El-Masry. Appl. Phy. Letters, 70 1647-1649 (1997), https://doi.org/10.1063/1.118658.
17. Yangfong Huang, YebinCai, Dongkai, Qiao and Haoliu., Particulogy9, 170-173(2011), https://doi.org/10.1016/j.partic.2010.07.023.
18. S.Parvathy and B.R.Venkatraman. Journal of Environmental Nanotechnology,64 31-34 (2017).
19. M. Farahmandjou, M. Zarinkamar and T.P. Firoozabadi. Revista Mexicana De Fisica, 62, 496–499 (2016). https://www.scielo.org.mx/scielo.php?script=sci_arttext&pid=S0035-001X2016000500496
20. Malatesh S Pujar, Shirajahammad M Hunagund, Delicia A Barretto, Vani R Desai, ShivaprasadagoudaPatil, Shyam Kumar Vootla and Ashok H Sidarai., Bull. Mater. Sci., 43, 24 (2020).
21. Mahsa. Zarinkamar, Majid. Farahmandjou and Tahereh. PormirjafariFiroozabadi. Journal of Ceramic Processing Research, 13, 166-169 (2016),
22. R.Suresh, V. Ponnuswamy and R. Mariappan. Applied Surface Science, 273 457-464 (2013).
23. S.A.H. Tabrizi, M. Mazaheri, M. Aminzare and S.K. Sadrnezhaad. Journal of Alloys and Compounds, 491, 499–502(2010), https://doi.org/10.1016/j.jallcom.2009.10.243.